Integrated Power/Attitude Control System (IPACS)

J. E. Notti,* A. Cormack, † and W. J. Klein‡
Rockwell International Corporation, Downey, Calif.

An integrated power and attitude control system (IPACS) for spacecraft is described. The system utilizes energy wheels for electrical energy storage as well as attitude control. Results from the feasibility studies of this concept are summarized and indicate potential weight and cost savings up to 30% over conventional power and control systems. The IPACS advantage is particularly significant for the longer duration missions which have a large number of energy charge-discharge cycles and higher power requirements. A system for a shuttle-launched Research and Applications Module (RAM) free-flying observatory spacecraft is described. The system utilizes three gimbaled, control, and energy-momentum gyros in a planar array. Each gyro unit is rated at 2.4 kw and delivers 1095 w-hr of energy while maintaining control angular momentum above 1115 N-m-sec. Dynamic response of combined power and control functions was evaluated by digital simulations which included significant nonlinearities and a symmetrical energy distribution law. Simulation data indicate that spacecraft attitude control response is similar to that achieved without the superposition of energy wheel speed changes and is essentially uncoupled from that of the faster power control loop. Both power and control dynamics are well regulated.

I. Introduction

A NUMBER of spacecraft designs have been developed for the missions of the shuttle era. Most of these require subsystems with lifetimes of 5-7 yr to meet cost effectiveness goals. Pointing requirements below 0.25° are common, with specific scientific missions requiring experiment pointing to 1 arc sec. Momentum storage devices normally are used to provide control torques for long-life missions where control thruster propellant weights and valve life test costs prove excessive. The choice of momentum storage is reinforced, or even required, in several missions where mass expulsion contaminants are prohibited by experiment viewing requirements or where fine pointing stability and slewing is required.

The significant impact of the long-life requirement on the electrical power system design is in the sizing of components rather than in the type of system selected. This is because nearly all systems postulated utilize solar arrays for electrical power generation and secondary batteries for electrochemical energy storage. The batteries prove to be the heaviest components of advanced spacecraft solar power systems. The weight of the batteries is determined by the rated energy densities and their inherent characteristic of decreasing life with increased depth-of-discharge and charge-discharge rate. Thus, for a specific energy storage requirement, the designer's major option for increasing battery life is that of increasing the size or number of battery cells thereby decreasing the depth of discharge. As a result, batteries and their controllers commonly constitute 30-40% of an electrical power system weight.

Developments of recent years[1,2] have shown that flywheels designed to store energy can provide higher energy densities than can be expected from several conventional spacecraft electrochemical devices. In spacecraft applications, parity in energy density between the energy wheel and battery subsystems may result in significant advantage to the energy wheel system. This is because many spacecraft designs currently employ flywheels in momentum storage attitude control systems which approximate the weight of energy wheels. Thus, an energy wheel subsystem designed to perform the dual functions of electrical energy and momentum storage can provide significant weight advantage through deletion of batteries and associated power control electronics. As defined herein, flywheels designed to perform the dual functions are termed energy-momentum wheels.

Presented as Paper 74-921 at the AIAA Mechanics and Control of Flight Conference, Anaheim, California, August 5-9, 1974; submitted August 28, 1974; revision received February 24, 1975.

Index categories: Spacecraft Attitude Dynamics and Control; Spacecraft Electric Power Systems; Earth Satellite Systems.

*Supervisor, Space Division. Member AIAA.

†Project Engineer, Space Division.

‡Staff Engineer, Space Division.

II. The IPACS Concept

The integrated power and attitude control system consists of solar cell arrays, energy-momentum wheel subassemblies, gimbals, gimbal actuators and sensors, and all control electronics associated with electrical power conditioning and attitude control functions. Figure 1 illustrates the system concept. Electrical power is supplied directly from the solar array to the loads through a regulated spacecraft bus. Electrical energy is stored by accelerating the flywheels during the orbit day and discharging to the spacecraft bus during peak load and orbit night periods. Spacecraft attitude control is accomplished simultaneously by changing the momentum state of the flywheels.

Momentum changes for attitude control torque generation can be accomplished by conventional means. The energy-momentum wheels are used in either a reaction or gimbaled configuration. In the nongimbaled mode, reaction energy wheels (REW), are configured in momentum-canceling pairs or arrays which accelerate and decelerate in unison to provide

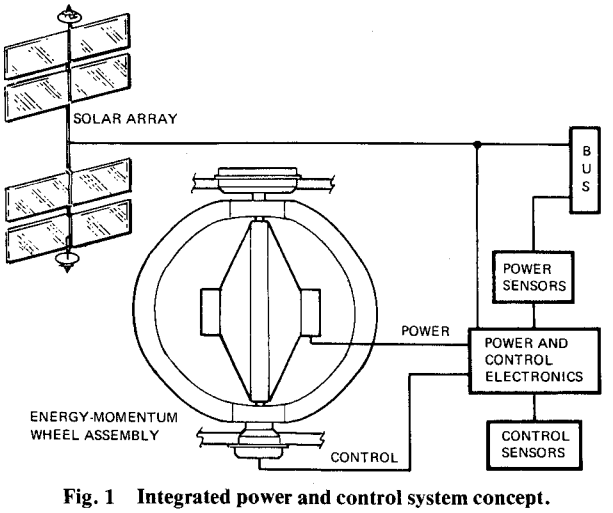

Fig. 1 Integrated power and control system concept.

Table 1 Representative mission requirements

Mission				Control			Power		
							Energy Storage		
Spacecraft	Mission duration	Orbit altitude (km)	Spacecraft weight (kg)	Pointing accuracy (Rad)	Control torque (N-m)	Momentum storage (N-m-sec)	Charge/discharge cycles	Energy/cycle (w-hr)	Power output (w)
RAM	5 yr	500	12,200	4.85×10^{-6}	9.5[a]	2034 (planar)	27,800	2,500	4,800
TDRS	3 yr	35,700	1,230	0.016	0.021[b]	16.9 (bias)	450	285	237
EOS	2 yr	1,100	770	0.017	0.049[b]	24.4 (bias)	10,200	460	1,048
MJS	4 yr	9.5 a.u.	680	0.00087	0.014[b]	0.068	10	360	20
MSS	10 yr	500	81,500	0.0044	678[b]	2758 (planar)	52,600	14,900	20,000
Shuttle sortie	30 days	185	97,500	0.0087	163[a]	7118 (planar)	10,000	6,100	61,000
Shuttle ATL	7 days	185	97,500	0.0087	163[a]	7118 (planar)	2,000	1,090	1,900

[a]Per torquer. [b]Per axis.

Table 2 IPACS characteristics

	RAM	EOS	MSS	Shuttle 30-day	TDRS	MJS	Shuttle ATL
Wheel array	3 double-gimbaled (planar)	4 opposed nongimbaled	5 skewed, single-gimbaled	3 double-gimbaled (planar)	4 opposed nongimbaled	4 skew nongimbaled	3 double-gimbaled (planar)
Energy per wheel (w-hr)	1095	173	3730	3050	71	90	975
Power rating per wheel (w)	2410	525	5000	30,500(gen) 2000 (motor)	120	12.5	1200
Maximum speed (rpm)	45,000	60,000	35,000	35,000	50,000	100,000	18,500
Wheel array weight (kg)	225	52	730	675	26	17	325
Bearing type	Ball	Active magnetic suspension	Active magnetic suspension	Active magnetic suspension	Ball	Active magnetic suspension	Ball

energy and allow relatively small residual control momentum vectors. The gimballed units, control-energy momentum gyros (CEMG), cycle between maximum and minimum momentum states providing control torques in the same manner as conventional control-moment gyros. The maximum momentum is the result of the energy requirement, while the minimum momentum is the value required for effective control.

The central power and control electronics provide electrical power conditioning and regulation as well as attitude control sensor processing, shaping, command generation, and mode control. The energy-momentum wheels are powered by motor-generators with dynamic response which allows bus regulation. Power is regulated by bus and reference voltage differencing which switches the units between the motor and generator modes.

The energy-momentum wheels can be designed to operate as conventional momentum storage control devices for a portion of the mission, with on-orbit switching to higher speed and simultaneous energy-momentum operation for the remainder. The wheels also can be configured to perform only a portion of the total energy storage function of an electrical power system. As defined herein, IPACS performs the total energy storage function and utilizes no batteries, chargers, charger control electronics, or amp-hr meters for on-orbit operations.

III. Feasibility Studies

The feasibility of the IPACS concept has been studied by the Rockwell International Space Division for NASA's Langley Research Center.[3] The objectives of the study were: 1) to determine the feasibility and cost-effectiveness of a solar array energy wheel system capable of dual functions of spacecraft electrical energy storage and attitude control; 2) to establish the boundaries of application of this system for both manned and unmanned spacecraft; 3) to identify hardware components considered critical to the viability of the concept, and to define the level of development required; and 4) to generate preliminary designs for two specific spacecraft to be selected at the conclusion of the feasibility analysis.

A survey of various NASA mission models through 1990 resulted in the selection of seven spacecraft missions which were considered representative of the major mission classes: a low-orbit satellite (Earth Observations Satellite-EOS); a geosynchronous vehicle (Tracking and Data Relay Satellite-TDRS); a planetary spacecraft (Mariner Jupiter/Saturn-MJS); an extended duration (30-day) shuttle sortie mission; a free-flying shuttle research and applications module (RAM); a modular space station (MSS); and a seven-day shuttle sortie mission with the Advanced Technology Laboratory (ATL) payload. Major mission, electrical power, and attitude control requirements of the seven missions are shown in Table 1.

Table 3 Comparison Summary of IPACS and Conventional Systems

Spacecraft	Volume (m^3)		Weight (kg)		Momentum (N-m-sec)		Cost savings (%)
	IPACS	Conventional	IPACS	Conventional	IPACS	Conventional	
TDRS	0.08	0.03	86.9	96.9	16.9	16.3	11
MJS	0.02	0.006	161.7	154.9	...	...	Penalty
ATL	0.5	0.33	1200.2	1477.8	2374	3118.8	4
30-day Shuttle	0.3	1.9	3205	3420	3932	3118.8	Penalty
RAM	0.08	0.4	1117	1615	1115	678	30
MSS	0.53	4.9	6043	7118	4990	4475	2

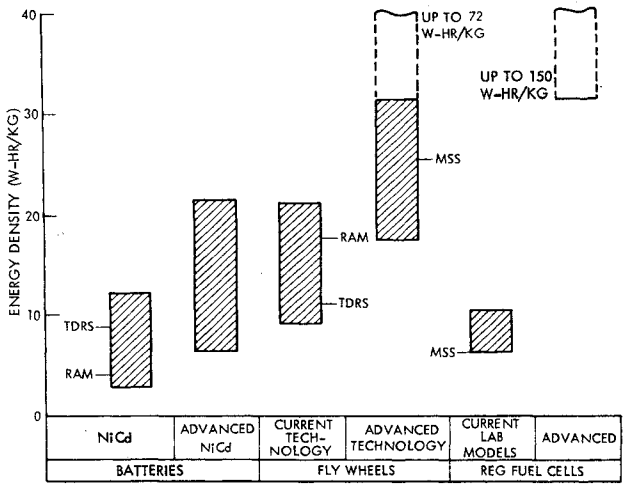

Fig. 2 Energy storage subsystem capability and potential.

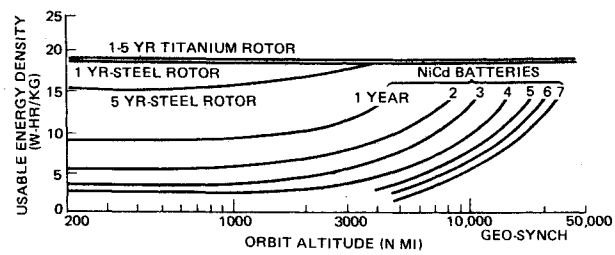

Fig. 3 Energy density variation with orbit altitude and mission duration.

Feasibility was evaluated by comparing the physical, performance, and cost characteristics of candidate IPACS designs with the characteristics of conventional electrical power and attitude control systems. The conventional systems selected for comparison with IPACS were NASA-approved designs resulting from previous Phase B contracts. Comparisons were made at comparable technology levels and cost comparisons were performed with the same estimating relationships. The feasibility studies and simulations showed that simultaneous electrical energy storage and attitude control by means of flywheel arrays appeared technically feasible for all missions studied. Both electrical power and attitude control performance requirements can be satisfied by high-speed flywheel energy-momentum units utilized in gimbaled or nongimbaled arrays.

Table 2 summarizes the major characteristics of the selected IPACS configurations. Analyses confirmed that each system met the performance requirements of Table 1. In Table 3, comparison factors between IPACS and conventional designs are summarized.

The IPAC systems are predicted to weigh less than conventional systems for all missions except the planetary. The low energy storage requirement of the planetary mission coupled with only a few discharge cycles at planet encounter resulted in a prohibitive flywheel system weight penalty. The weight advantage in the other missions approximates the weight of the batteries deleted. Although energy-momentum wheels generally weigh somewhat more than their conventional momentum-exchange counterparts, the energy density advantage of the wheels as compared with batteries compensates to allow a net system weight reduction.

The effect is illustrated in Fig. 2, which is representative of the range of expected energy densities for spacecraft energy storage subsystems. Values shown represent usable energy at the subsystem output, including losses and weight of ancillary equipment. The data ranges were developed utilizing a fixed 50% speed reduction and 46-70 w-hr/kg rotors for the current and advanced technology designs, respectively. Current-technology flywheel systems employing isotropic rotors and conventional ball bearings are shown to compare well with advanced nickel cadmium (NiCd) batteries. Advanced-technology flywheel units employing composite rotors and noncontact magnetic suspension bearings are estimated to exceed advanced NiCd batteries and regenerative fuel cell technology which has been demonstrated but not qualified. Advanced regenerative fuel cell technology is expected to have development costs higher than other systems shown. If rotor energy densities were to reach the 135-145 w-hr/kg values predicted by some researchers, the dashed lines of Fig. 2 would show the advanced flywheel values comparable to the predictions for advanced fuel cells.

Reference points which show the specific values for the conventional and IPACS energy storage designs are shown. It should be noted that whereas the range for battery densities is primarily affected by charge-discharge cycles, the flywheel density variations depend more on material selection and speed reductions. This relative insensitivity of IPACS to mission cycles is illustrated in Fig. 3, where a conventional NiCd subsystem is compared with current-technology IPAC subsystems with two different rotor materials.

The rotor materials shown both have comparable delivered energy density at the subsystem level and are relatively insensitive to orbit altitude (charge-discharge cycles) for one-year missions. The strength-to-density ratio values are similar for both materials at a low number of stress cycles. As stress cycles increase the titanium rotor has a clear fatigue life advantage. Both systems can achieve higher energy densities than the NiCd subsystem. The data shown for NiCd batteries are based on a 56.7-kg energy storage subsystem having a 1000 w-hr capacity (100% depth of discharge).

The studies also showed IPACS to have higher storage efficiency than the conventional systems. Figure 4 shows data for four representative missions. The efficiencies were calculated for the baseline solar array voltages which, in general, were below the optimum IPACS rated voltage. The motor generator electronics can achieve higher efficiencies at a higher array voltage. The potential exists for further reductions in power distribution and solar array weight by optimizing array voltage and rated power for each IPACS unit. The feasibility studies also included an analysis of application boundaries and cost-effectiveness.

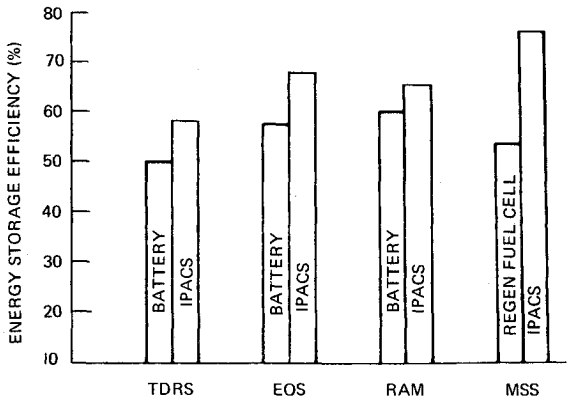

Fig. 4 Charge-discharge efficiency.

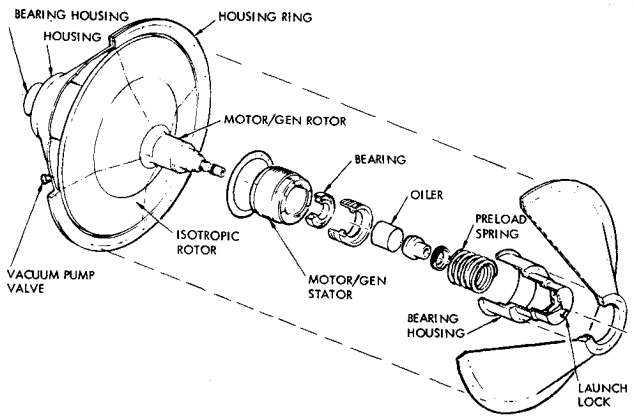

Fig. 5 Current technology energy-momentum wheel.

The studies also showed IPACS to have higher storage efficiency than the conventional systems. Figure 4 shows data for four representative missions. The efficiencies were calculated for the baseline solar array voltages which, in general, were below the optimum IPACS rated voltage. The motor generator electronics can achieve higher efficiencies at a higher array voltage. The potential exists for further reductions in power distribution and solar array weight by optimizing array voltage and rated power for each IPACS unit.

The feasibility studies also included an analysis of application boundaries and cost-effectiveness. The studies did not show any inherent power, energy, or control boundaries which limit IPACS in spacecraft appliations. Power levels to 80 kw and energy storage to 70 kw-hr are obtainable for designs sized to spacecraft dimensional constraints. Attitude control dynamic range and pointing accuracy is expected to approximate that of current control-moment gyros.

Cost-effectiveness was evaluated by comparing estimated costs of IPACS designs with the original cost estimates of the designs for the conventional power and control subsystems. IPACS appeared competitive for all missions except the planetary MJS mission and the particular 30-day shuttle sortie mission studied. The shuttle mission was characterized by a short-term 60-kw power requirement for a few cycles. The planetary mission was characterized by a low energy storage requirement for three discharge cycles at planet encounter. In both cases, IPACS development costs exceeded costs of a short-life, high-energy-density battery system. IPACS was shown to promise significant cost advantages for spacecraft with extended life missions or a recurring mission usage such as the RAM and ATL shuttle missions. In general, IPACS development costs were similar to those required for conventional systems and operational costs significantly better by reason of its lower weight, predicted life, and refurbishment advantages.

At the conclusion of the feasibility studies, preliminary designs were prepared for the TDRS satellite and RAM free-flying spacecraft. The energy-momentum wheel assembly for the RAM design is now being developed by Rockwell International for design verification tests and flight simulation by the NASA Langley Research Center.

IV. RAM Requirements

The objective of free-flying RAM A303B mission is to accomplish solar astronomy observations. Experiments include photoheliograph, UV spectroheliograph, solar X-ray telescope, and solar coronograph experiments.

The vehicle is delivered to orbit by the shuttle. The desired orbit is circular with an inclination of less than 10° and an altitude of 740 km. Acceptable orbit characteristics are a circular orbit with an inclination between 45 and 55° and an altitude of 500 km. Mission duration is five years. Free-flying RAM spacecraft are to be designed to facilitate their retrieval and recovery by the shuttle in case of the failure of critical onboard systems. The vehicle will be designed for in-orbit maintenance in a shirtsleeve environment with a nominal service interval of six months. The vehicle is manned periodically for in-orbit servicing but nominally operates unmanned.

Attitude Control Requirements

The nominal vehicle flight mode will be solar inertial with the longitudinal axis of the vehicle oriented toward the sun. Experiment-integral sensing will be provided. The aspect or error signal so obtained will be used for vehicle control. The vehicle will be controlled to a pointing accuracy of 1 arc sec. The experiment required pointing stability is 0.017 arc sec over the observation period which is considered as 45 min. It is acceptable for the vehicle to be controlled to a stability of 0.5 arc sec with the experiment providing the finer stability. During experiment observations, the experiment must not be subjected to acceleration levels greater than $1 \times 10^{-4}g$'s. The predominant external disturbances are aerodynamic and gravity gradient. The worst-case momentum storage requirement including maneuvers is 2039 N-m-sec. The requirement of the conventional design was to revert to RCS with any single failure. This requirement was applied to the IPACS design.

Electrical Power Requirements

Total power requirements are obtained by adding payload and subsystem (1020 w) requirements. An average total load power of 3400 w is shown by the RAM Phase B study for the A303B payload. The experiment loads require 1000 va of 115/200 vac power and 1.5 kw of ± 5% regulated 28 vdc power.

At 500-km orbit altitude, the eclipse energy required by spacecraft loads is 2010 w-hr. This is based on an eclipse period of 0.591 hr. A 5-yr mission will require 27,800 charge-discharge cycles.

V. System Description

Major assemblies making up the RAM IPACS are the solar array panels, energy-momentum wheel assemblies and associated electronics, central control unit, and the regulated bus. The mechanization is based on minimum modification of the conventional RAM power regulation and distribution system.

The three double-gimbaled CEMG units replace the three double-gimbaled CMG's in the conventional attitude control design. The remainder of the baseline control concept is retained including the sensors, RCS, magnetic torquers for desaturation, and reaction wheels for precision control. The three CEMG's replace eight 36-AH (24-cell) nickel cadmium batteries. Figure 5 illustrates a CEMG inner gimbal design with specific parts omitted for clarity.

The constant-stress wheel is fabricated of steel, weighs 44 kg, and operates over a speed range of 22,500 to 45,000 rpm.

Angular momentum varies from 1114 to 2229 N-m-sec and stored energy from 365 to 1460 w-hr over this speed range.

The rotor is supported on two precision angular contact ball bearings. The bearings are preloaded by a long travel spring. Centrifugal oilers, having a 5-yr storage capacity, are used to lubricate the spin bearings.

To provide a maximum of 2400 w output from the rotor, two permanent-magnet, brushless motor-generator units are used. These are identical, two-pole machines especially designed for 96-97% efficiency. The motor-generator rotor is contained within the shaft of the wheel and utilizes rare earth magnets of high coercive force.

The wheel enclosure and inner gimbal is an aluminum double conical structure giving high stiffness and minimum weight. A central ring supports the gimbal shafts and provides the mounting surface for each gimbal cone. Electronics for the motor-generator are mounted on the inner gimbal assembly to minimize the number of flexible leads.

The total weight of the inner gimbal assembly is 56.1 kg. The assembly is 41.9 cm in diameter and 44.2 cm along the spin axis. Table 4 presents a summary of the total integrated power and control system. The system shows a weight saving of 498 kg over the conventional system which utilized 442 kg of battery energy storage.

The three CEMG's are mounted in the vehicle in a planar array with the outer gimbal axes parallel and aligned with the longitudinal axis of the vehicle, which is the minor inertia axis. Thus the three outer gimbal torques act in parallel. The deliverable torque about the transverse axes depends on the instantaneous gimbal configuration but in general will be equal to or greater than the output of a single torquer.

Energy is stored in all three wheels under normal operating conditions. Under failure mode conditions, the two remaining units are slewed to a position where the spin axes of the rotors are colinear. The rotors are counter-rotated to provide energy storage. The primary attitude control function is assumed by the reaction control system supplemented by the CEMG's.

When power demand exceeds solar array capability (daylight peaking or orbit eclipse periods) the bus voltage will drop below a deadband about the nominal value of 28 vdc. The power control unit will modulate the generator electronics to supply the additional power needed. During daylight periods when solar array power exceeds load requirements, the power control unit will apply power to the motors to increase rotor speed, if they are not already at maximum rpm (45,000).

The nominal eclipse power required from the generators including bearing losses is 4440 w. This can be supplied by two CEMG's with generators operating at about 93% of full output. Nominally, all three units will operate simultaneously to deliver eclipse power at 1540 w per wheel. A minimum of two CEMG's is required to meet eclipse power requirements. However, all three CEMG's will be needed to meet eclipse energy requirements. The total eclipse energy requirement from the array is 2743 w-hr. Available energy from all three CEMG's is 3285 w-hr. (for a speed reduction from 45,000 to 22,500 rpm). Therefore 87% of total stored available energy is used to meet eclipse power requirements.

VI. Simulation Description

Effects of energy transfer coupling with CEMG control performance were investigated by digital simulation. The system model shown in Fig. 6 consists of four functional parts: 1) CEMG configuration; 2) torque control law; 3) energy control law; and 4) attitude control loops.

Gyros are identical and modeled to include significant friction and dynamics. Static friction acts as a breakout force threshold for gimbal motion while running friction functions as a braking force on the relative motion between a gimbal and its case. Viscous damping is not included since its effect is negligible.

Gimbal motors are represented by gains while the motor

Table 4 RAM IPACS weight summary

Subassemblies	Weight (kg)
Solar array	256
Power conditioning and distribution	152
Power and momentum controller	10
CEMG's (3)	225
Baseline control retained	180
Wiring and mechanical	294
Total	1117

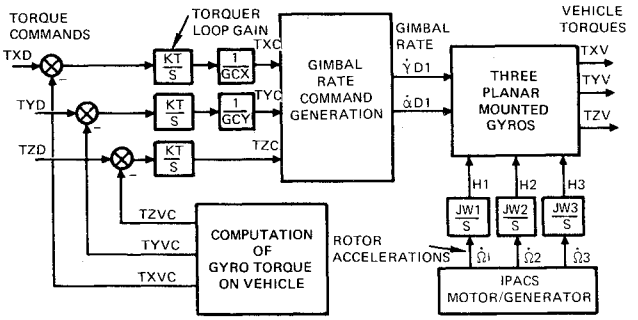

Fig. 6 Torque and energy control model.

torques are developed in response to gimbal rate commands summed with shaped tachometer signals. The signal mixing acts to null the precession torques due to gimbal rates and thereby decouple inner and outer gimbal motion. Gyro torques on the spacecraft are the result of the contributions of the three CEMG's.

The desired operation of the gyro array is to make its vector rate of change of angular momentum coincident with the commanded torque vector. Torque feedback with modified transpose gain distribution for generating gimbal rate commands was selected as the control law to be used. It meets general control law objectives of 1) predictable and acceptable system transient response, and 2) maximum utilization of gyro momentum.

For the RAM model, torque command errors are formed by differencing the commanded torque and the developed torque. The transpose of the gimbal angle transformation operates on these signals to generate gimbal rate commands for the CEMG's. An inner tachometer feedback loop is used to minimize gimbal wander occasioned by gimbal system nonlinearities such as friction forces. The selected mechanization features an integrator at the input to the command distribution matrix. This permits a sufficiently large torque motor gain to increase the motor-tachometer loop cross-over frequency and assures a fast inner loop without interaction with outer-loop cross-over frequencies.

Energy is transferred into or out of the control system by changing the speed of the wheels. The energy command is formed by a voltage control loop operating from the spacecraft bus which drives the motor-generators. Simulations were used to verify that the bandpass of the voltage control loop can be adjusted well over a decade above the primary control-loop frequency. The power return simulation is then dynamically uncoupled from that of primary control and is represented by acceleration commands to the wheels as derived from representative power profiles. A simple energy distribution law which presumes the energy transfer rate is equally distributed among the wheels of the three gyros proved effective.

Gyro array torques about each spacecraft control axis are

summed with the zero energy torque terms and serve as the total torque feedback signals. The outer control loops comprise conventional attitude and attitude rate feedback loops. Although a simple spacecraft model is used, the computer simulation is formatted to accommodate flexible body modes and additional system nonlinearities.

VII. Simulation Results

The CEMG digital simulation described was used to determine system energy storage and attitude control performance based on representative RAM spacecraft and gyro properties as presented in Table 5. Before simulating the RAM IPACS for the more stringent operating conditions, a linear analysis was used to establish nominal control system gains to satisfy the following criteria: 1) single-axis response shall approximate a second-order system with a 0.7 damping ratio; and 2) single-axis response shall be identical for each control axis. The break frequency of the tachometer loop was set at 50 rad/sec to provide the fast inner loop needed to minimize the effect of gimbal motion nonlinearities. Control frequencies for the nominal system gains are approximately 1 and 24 rad/sec, adequate separation from the 50 rad/sec inner loop.

Nonlinear system simulation runs, using the linear system gains and initial conditions, were made to determine the effects of friction on single-axis response. Values of 0.0237 N-m were used as estimates of static and running friction torques for direct-drive brushless gimbal torque motors. Comparison of linear and nonlinear response indicates that gimbal friction of this magnitude has virtually no effect on spacecraft attitude response. However, nonlinearities are evidenced in vehicle torque and other inner loop variables. As expected, nonlinearities are noticeable (Fig. 7) whenever a near-zero gimbal rate exists and gimbal motion is inhibited by the static friction breakout torque. Peak values of mission-critical variables, notably gimbal motor torques, are not significantly increased by the effects of gimbal friction.

Torque on the vehicle due to the effect of wheel speed change and the distribution of such torque about individual vehicle control axes depends on the gimbal angle of the gyros as well as the speed change magnitude. The array momentum at any time depends on previous momentum history. Various simulation runs were made to explore the impact of initial momentum state upon response data. The ability of the control system to satisfy the 1 arc sec attitude control accuracy requirement is illustrated in Fig. 7 with time histories showing

Table 5 RAM data base

Maximum energy charge state	
Charge rate	7221 w
Rotor acceleration	2.16 rad/sec^2
Rotor speed	22,500 rpm
Maximum energy discharge state	
Discharge rate	4820 w
Rotor deceleration	0.72 rad/sec^2
Rotor speed	45,000 rpm
Spacecraft moments of inertia	
Roll axis	159850 N-m-sec^2
Pitch axis	163100
Yaw axis	29950
CMG characteristics	
Rotor inertia	0.473 N-m-sec^2
Inner gimbal inertia	0.271
Outer gimbal inertia	0.354
Peak gimbal motor torque	9.49 N-m

Table 6 RAM simulation conditions

Item	Property
Initial gyro array state	
X, Y: plane momentum	2034 N-m-sec
Z momentum	407 N-m-sec
Wheel speed	22500 rpm
Inner gimbal angles	6.98 deg
Gyro 1 outer gimbal angle	0 deg
Gyro 2 outer gimbal angle	−54.8 deg
Gyro 3 outer gimbal angle	54.8 deg
Forcing functions	
Energy charge rate per wheel	2407 w
Yaw attitude initial error	0.01 deg

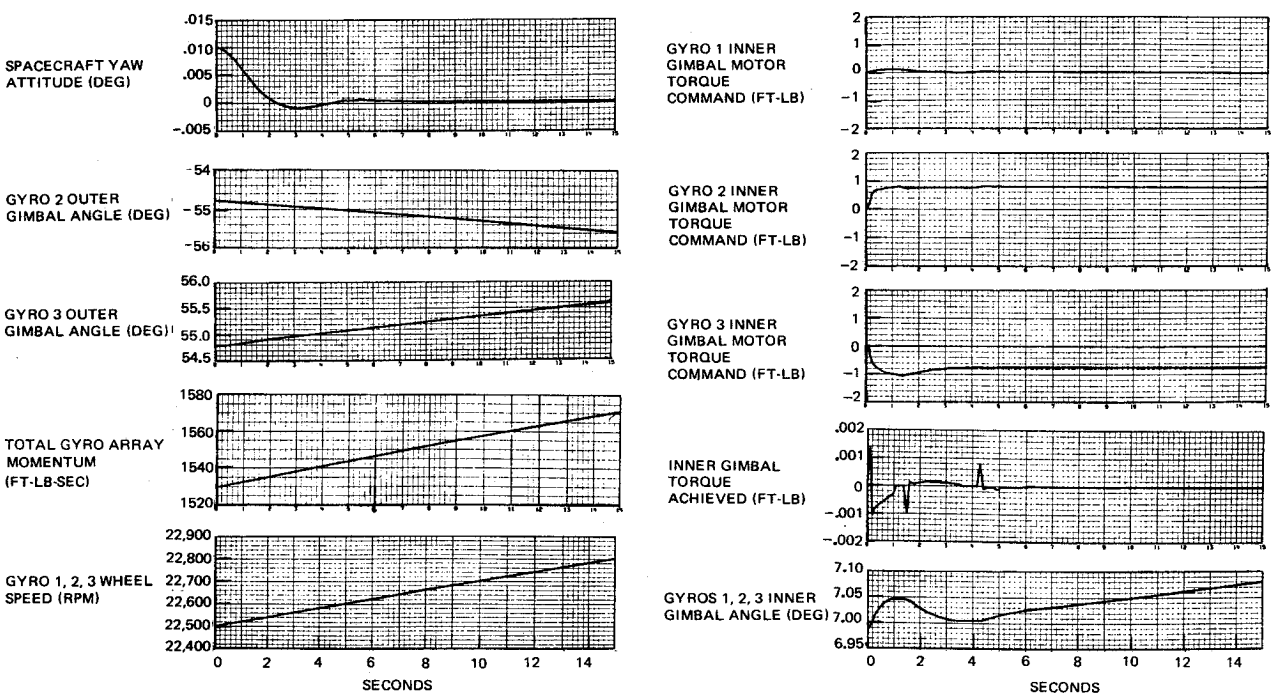

Fig. 7 RAM IPACS simulation—maximum energy charge rate and yaw attitude command.

a maximum energy charging rate plus a yaw attitude command. Forcing functions and initial state values of the gyro array for the time histories presented are listed in Table 6. These data indicate attitude error is reduced to less than 1 arc sec in less than 10 sec. Outer gimbal motor torques are identical and the relative outer gimbal angle change is smooth. Energy coupling is seen in the inner gimbal torque commands with the command for gyro number three of opposite polarity. Achieved inner gimbal torques with the coupling, however, is seen consistent and inner gimbal angles of the three gyros track for the yaw maneuver. Conclusions based on simulation results are summarized as follows.

1) Response for combined energy and control conditions approximates the control-alone case with system sizing and gain selection accomplished by conventional techniques.

2) Simulation data show that CEMG attitude control dynamics can be determined analytically by linear analysis. Constant control system gains can be utilized with shaping for changing momentum states not required.

3) Representative gimbal friction nonlinearities do not appreciably affect system dynamic response characteristics.

4) Maximum gimbal motor torque during energy charge conditions does not exceed 50% of maximum rated motor torque for any expected conditions, thus leaving an adequate margin for countering disturbance torques. The peak motor torque is experienced during the few seconds following initiation of energy transfer operations. The effect on controlling vehicle attitude is negligible, since attitude errors are reduced to near-zero conditions within 10 sec after onset of energy transfer torque.

VIII. Conclusions

Feasibility studies have shown that the use of energy-momentum wheels in an integrated power and control system configuration can result in significant weight and cost savings to future spacecraft. The advantages of this type of system appear particularly significant for the longer duration missions characterized by a large number of charge-discharge cycles at power levels above 1 kw. No technical limitations in the application of IPACS to spacecraft of the NASA mission models were uncovered. IPACS did not appear cost-effective, however, for missions with low energy storage requirements. The design of a 2.4-kw gimbaled unit has verified many of the technical conclusions of the feasibility study and would promise a power and control subsystem weight decrease of 30% for a free-flying RAM spacecraft in low earth orbit. Simulation results have shown control interaction of the energy function to be minimal.

References

[1] Helsley, C.W., et al., *"Energy Storage Substation Concepts for Aircraft Actuation Functions,"* Tech. Rept. AFAPL-TR-66-29, Air Force Aero Propulsion Lab., Wright-Patterson Air Force Base, Ohio.

[2] Rabenhorst, D.W., *"Potential Applications of the Super Flywheel,"* Presented at the Intersociety Energy Conversion Engineering Conference, Boston, Mass., 1971.

[3] Notti, J.E., et al., *"Integrated Power/Attitude Control System (IPACS) Study;* Vol. 1- Feasibility Studies." CR 2383 April 1974, NASA.

[4] Rabenhorst, D.W., *"Primary Energy Storage and the Super Flywheel,"* Johns Hopkins University, Tech. Memo. TG 1081 Sept. 1969.